Journal of Thermal Science and Technology

Vol. 3, No. 3, 2008

# Study on Low Directivity Condensing Equipment for Solar Power Collection Based on a Single Leaf Shoot Shape*

Shin'ya OBARA**, Itaru TANNO** and Taichiro SHIRATORI**

**Tomakomai National College of Technology,
Nishikioka 443, Tomakomai, HOKKAIDO 0591275, Japan
E-mail: obara@indigo.plala.or.jp

**Abstract**

The distribution of solar cell modules is planned by referring to the configuration of plant shoots. The object is to develop a solar power generation system with low directivity and a small installation space. In this paper, the amount of insolation that reaches a plant shoot in an arbitrary period was investigated using the "Light received analysis algorithm of a plant shoot" (LAPS) described in a previous report. Based on the analysis, the optimal configuration of the shoot to maximize the amount of light received was determined. The position of the light source on a representative day in summer has a wide range of elevation angles and directions, and has a narrower range in the winter. This paper mainly examines the condensing system of low directivity using the plant shoot of a simple leaf. Based on the relation between the characteristics of these light sources, the shoot configuration for the summer season is optimized by a solar position at 12:00, with considerable solar radiation. The shoot configuration for winter, meanwhile, is arranged so that half the total leaves may absorb solar radiation at a small elevation angle. When the amount of light received by the leaves arranged horizontally and the optimized plant shoot configuration for every month is measured, the difference is found to be modest during the period from March to September. However, a greater amount of light is received in the plant shoot arrangement in January, February, and October to December, based on an optimal solution that is superior to that with the leaves arranged on the level surface.

***Key words***: Solar Energy, Solar Power Generation, Genetic Algorithm, Leaf Arrangement Analysis, Plant Shoot

## 1. Introduction

Many plants are dependent on carbohydrates obtained by photosynthesis for energy. Therefore, in a forest with many competitors, it is thought that the leaf shape, as well as the arrangement and orientation of many plants, are designed so as to maximize the photosynthetic rate. The branches and leaves in low positions, which sunlight does not reach easily, do not grow in many cases. In individual plants, this tendency is especially remarkable [1]. In this study, the relation between various plant configurations and the amount of light received is investigated, and a solar power generation system with a small installation space and modest influence of solar position is developed. We developed LAPS ("Light received analysis algorithm of a plant shoot") in order to investigate the configuration of a leaf and its relation to photosynthetic rate [2]. The Monte Carlo method and genetic algorithm (GA) are introduced into LAPS, and the characteristics of the light

*Received 7 Nov., 2007 (No. 07-0690)
[DOI: 10.1299/jtst.3.499]

received by a plant shoot (the group of one stalk and leaves, composed of a stalk, a leaf branch, and leaves) are investigated. The result of the numerical simulations using LAPS showed that the leaf form has a significant influence on the photosynthetic rate [2].

It is thought that, in a forest, a plant with many competitors has a configuration that allows considerable light to be received in a narrow space. Therefore, the distribution system of a solar module in the form of a plant shoot (DSMS) is examined. In this paper, the relation between the configuration of a plant shoot and the amount of light received is investigated using LAPS. This paper examines the condensing method with low directivity using the plant shoot of a simple leaf as a design. In the analysis, the sun is moved for every sampling time of the simulation via the virtual radiation surface. This paper expresses the variables concerning the position of the leaves by the chromosome model of GA using the parameters showing the plant shoot configuration. The magnitude of the amount of light received in a day defines the adaptive value of the chromosome model. The configuration of the plant shoot obtained by LAPS follows the objective of maximizing the amount of solar radiation. Therefore, a compact DSMS with weak directivity is proposed by using the LAPS method.

## 2. The distribution system of a solar module with the form of a plant shoot (DSMS)

2.1 Amount of light received by a plant shoot

A leaf is constructed of the shoot apex meristematic tissue of the stalk, and the leaf and stalk are joined by the leaf branch. In this paper, the unit of a plant shoot is considered to be composed of a stalk, a leaf branch, and leaves. Leaves are arranged on a stalk so as to maximize efficiency of photosynthesis. The space between a stalk and a leaf is also adjusted by the leaf branch. An example of a plant shoot and the optical system is shown in Fig. 1. Since the solar position changes over time, the angle of solar radiation relative to the plant shoot differs according to the sampling time. Therefore, in this paper, as shown in Fig. 2, the sun is simulated by defining the space coordinates of a virtual radiation surface. The positive direction of the x-coordinates indicates south. Solar radiation is simulated by emitting light perpendicular to the virtual radiation surface from a random position on the surface determined using the Monte Carlo method. The angle of elevation $\varphi_s$ and the direction angle $\theta_s$ of this virtual radiation surface are changed for every sampling time. On the other hand, as described in Section 3.1, the plant shoot configuration is expressed with the direction angle $\theta_t$, the elevation angle $\varphi_t$, the length of a leaf branch $r_t$, and the angle of rotation of the leaf $\beta$.

2.2 Directivity of the solar power generation system

If a weak-directive solar power generation system is realized, high power generation efficiency can be obtained, and is influenced by the solar radiation incidence angle. To date, the development of a spherical silicon solar cell [3] and a double-sided solar cell [4] have been used to reduce the directivity of a solar module. In this paper, DSMS with weak directivity is developed by optimizing the configuration of a plant shoot. The assumption is made that the amount of light received in terms of daily solar radiation is so large that the directivity of the acceptance surfaces is weak.

When the amount of light received is superfluous, the plant photochemistry system is damaged and water vaporization by a leaf also becomes superfluous. Under such circumstances, in order to avoid any reduction in the photosynthetic rate, a plant controls the amount of lighting via bending of the costa (Fig. 3). By applying a similar mechanism, a means of controlling the heat rise in a solar module may be possible. However, this paper does not describe this.

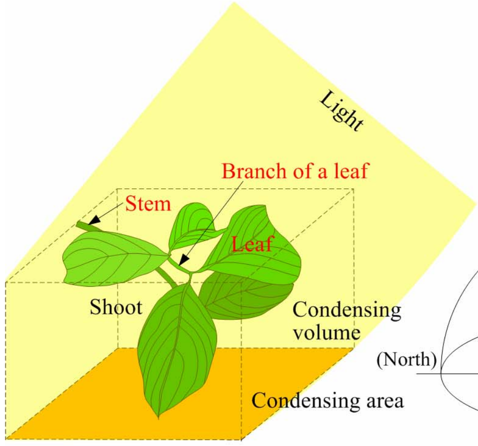


Fig. 1 Plant shoot and optical system

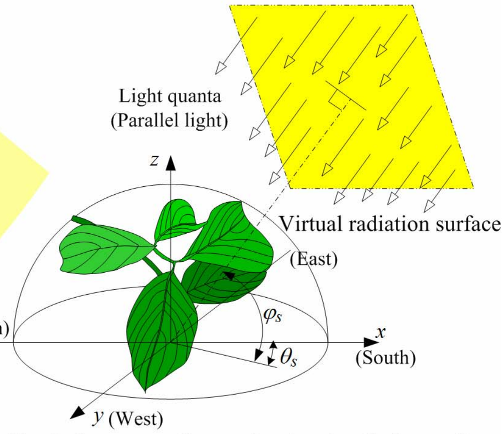


Fig. 2 Space coordinate of a virtual radiation surface


Fig. 3 Folding of a leaf

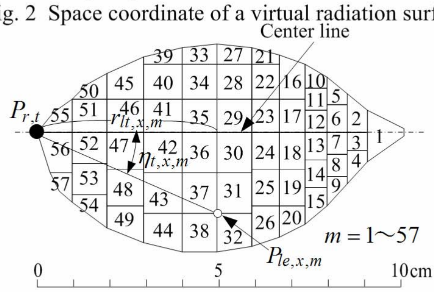


Fig. 4 Dogwood leaf model

2.3 Installation space and production of electricity

When introducing a solar power generation system in a city area or residential block, the installation site is generally restricted to rooftops. Since many solar modules installed in homes to date have been of the flat plate type, the production of electricity is dependent on the installation area. If solar modules with a plant shoot configuration are distributed, the production of electricity is proportional to the magnitude of the installation space. It is predicted that it would be easy to introduce the configuration of a plant shoot into a city area or residential block.

## 3. Analysis method using LAPS

3.1 Model

(1) The model of a plant shoot

The shoot configuration (the form of a leaf, direction and length of a leaf branch, etc.) are optimized by maximizing the amount of light received by a leaf and minimizing the overlap with other leaves. Although there are various types of plant shoots, a dogwood shoot is used as an example in this paper. Figure 4 shows the leaf model divided into 57 surface elements. Point $P_{r,t}$ is a corner point on the costa of a leaf. Subscript $t$ expresses the number of leaves. Each apex coordinate $P_{le,x,m}$ of the surface element of a leaf is given by an angle $\eta_{t,x,m}$ and a length $r_{lt,x,m}$, as shown in Fig. 4. Subscript $x$ is the apex number of a surface element, and $m$ is the surface element number. The photosynthesis capability of the leaf of a plant depends on the environmental condition of the light [1]. Therefore, the content of the photosynthesis enzyme $\varepsilon_{t,m}$ is designed to be given for every surface element $m$ of the leaf model $t$. In order to simplify the analysis, $\varepsilon_{t,m}$ of each surface element is set to be the same value.

The model of the shoot configuration of a dogwood is shown in Fig. 5. When there are two or more leaves, each leaf is similarly expressed as in Fig. 5. The positive $x$ direction indicates south, as in Fig. 2. Moreover, the reference planes of $\theta_t$ and $\varphi_t$ are the x-y and x-z planes, respectively, while the reference axis of $\beta_t$ is a line perpendicular to the x-y plane.

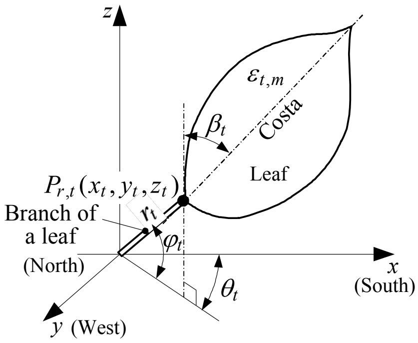


Fig. 5 Coordinate system of a shoot

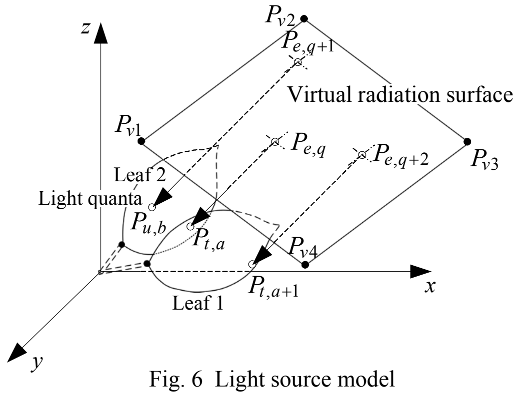


Fig. 6 Light source model

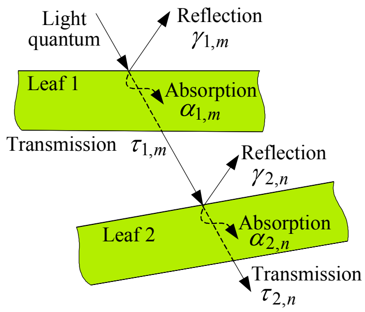


Fig. 7 Optical system model

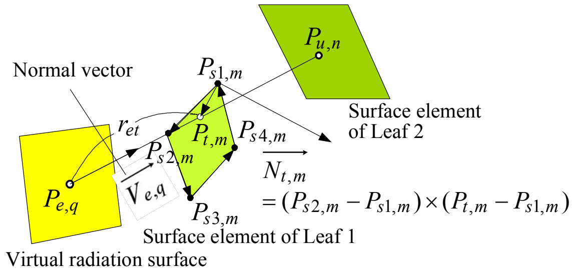


Fig. 8 Interrupt check of light quanta

(2) The model of the light source

Figure 6 shows the model of the virtual radiation surface with the emission of solar radiation. Solar radiation is emitted towards the leaves from a virtual radiation surface $P_{v,1}$ - $P_{v,2}$ - $P_{v,3}$ - $P_{v,4}$. Solar radiation is simulated with light quanta, and the photon flux density is calculated based on the number of light quanta arriving at each leaf using the Monte Carlo method. In this analysis, many light quanta are emitted to the leaves at right angles to the surface from the random point $P_{e,q}$ on the virtual radiation surface. The light quanta that directly reach Leaves 1 and 2 are expressed by $P_{t,a}$ and $P_{u,b}$, respectively. Subscripts $a$ and $b$ represent the numbers of the light quanta that reach Leaves 1 and 2 directly.

The number of light quanta $nq_{g,st}$ emitted during the sampling time $st$ of the representative month $g$ from the virtual radiation surface is calculated via the following equation, where, $N_a$ is the total number of light quanta emitted in a day, $R_{g,st}$ is the rate of the number of light quanta emitted by $st$, and $e_{g,st}$ expresses the amount of level surface global solar radiation during the period $st$ of the representative month $g$:

$$nq_{g,st} = N_a \cdot R_{g,st} = N_a \cdot \left( e_{g,st} \Big/ \sum_{st=0}^{Day} e_{g,st} \right). \qquad (1)$$

3.2 Shading check

Figure 7 shows the optical system model of the light quantum emitted from the virtual radiation surface. The light quantum passes the surface element $m$ of Leaf 1 before reaching the surface element $n$ of Leaf 2. The movement site of a light quantum can be determined by giving the reflectivity $\gamma_{1,m}$ of $m$, the absorptivity $\alpha_{1,m}$, and the transmissivity $\tau_{1,m}$ using the Monte Carlo method [5].

Figure 8 shows the method of checking the interception of solar radiation. The light quantum emitted from point $P_{e,q}$ on the virtual radiation surface passes the surface element $m$ on Leaf 1, and reaches the surface element $n$ on Leaf 2. The normal line vector of the arbitrary point $P_{e,q}$ on the virtual radiation surface is expressed with $\overrightarrow{V_{e,q}}$, where the symbol $\overrightarrow{\quad}$ expresses a vector. When the distance between $P_{e,q}$ and $P_{t,m}$ is expressed with $r_{et}$, the intersection coordinate $P_{t,m}$ on Leaf 1 will be calculated by Eq. (2). The symbol "・" in Eq. (2) expresses an inner product, and "×" in Eq. (3) expresses the outer product of a vector. When each side of Leaf 1 is expressed with a vector, the normal line vector in the apex $P_{s1,m}$ of the surface element can be calculated by Eq. (3). When $P_{t,m}$ as seen from $P_{e,q}$ is on the right side of all the side vectors, intersection $P_{t,m}$ exists within the surface element $m$ on Leaf 1. When $P_{t,m}$ is on the right side of side 1-2 of the surface element $m$, the conditions of Eq. (4) are satisfied. Likewise, checks are made as to whether $P_{t,m}$ is on the right side of all the sides.

$$P_{t,m} = P_{e,q} + r_{et} \cdot \overrightarrow{V_{e,q}} \tag{2}$$

$$\overrightarrow{N_{t,m}} = (P_{s2,m} - P_{s1,m}) \times (P_{t,m} - P_{s1,m}) \tag{3}$$

$$\{(P_{s2,m} - P_{s1,m}) \times (P_{t,m} - P_{s1,m})\} \cdot \overrightarrow{N_{t,m}} \geq 0 \tag{4}$$

$$\{(P_{s3,m} - P_{s2,m}) \times (P_{t,m} - P_{s2,m})\} \cdot \overrightarrow{N_{t,m}} \geq 0 \tag{5}$$

$$\{(P_{s4,m} - P_{s3,m}) \times (P_{t,m} - P_{s3,m})\} \cdot \overrightarrow{N_{t,m}} \geq 0 \tag{6}$$

$$\{(P_{s1,m} - P_{s4,m}) \times (P_{t,m} - P_{s4,m})\} \cdot \overrightarrow{N_{t,m}} \geq 0 \tag{7}$$

3.3 Amount of light received by a plant shoot

When the light quantum flux emitted from the virtual radiation surface reaches the surface element $k$ on leaf $w$, the number of arrivals is calculated from Eq. (8). The number of arrivals to $\dot{q}_{d,w,k}$ is the 1st term within the right-hand side bracket of Eq. (8). After transmitting to other leaves, the number of arrivals to $\dot{q}'_{h,i,k}$ is the 2nd term within the right-hand side bracket of Eq. (8). The position of the virtual radiation surface changes for every sampling time.

Equation (9) is a formula concerning $\dot{q}'_{h,i,k}$ on the right-hand side of Eq. (8). Here, $\tau_{j,m}$ is the transmissivity of the surface element $m$ of Leaf $j$. By multiplying the light quantum flux before transmission by the transmissivity, the number of light quanta transmitted to the surface element $m$ on Leaf $j$ is calculated. The transmission of a light quantum is determined by the Monte Carlo method using a random number between 0 and 1. The random number is compared with the transmissivity, and when the latter is larger, the light quantum is transmitted.

$$E_{w,k} = \sum_{t=0}^{N_a} \left( \dot{q}_{d,w,k} + \sum_{i=1}^{J_l} \dot{q}'_{h,i,k} \right) \quad (i \neq w) \tag{8}$$

$$\dot{q}'_{h,i,k} = \prod_{m=1}^{J_{e,i}} \left( \tau_{j,m} \cdot \dot{q}_{d,m,k} \right) \quad (j \neq w) \tag{9}$$

3.4 Analysis method

(1) Chromosome model

The chromosome model introduced into the analysis of GA is shown in Fig. 9. The chromosome model expresses $\theta_i$, $\varphi_i$, $\beta_i$, and $r_i$ with a 10-bit gene model of 0 and 1.

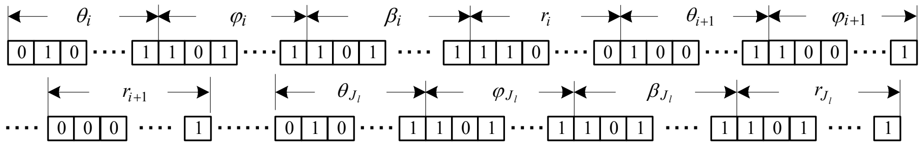

Fig. 9  Chromosome code

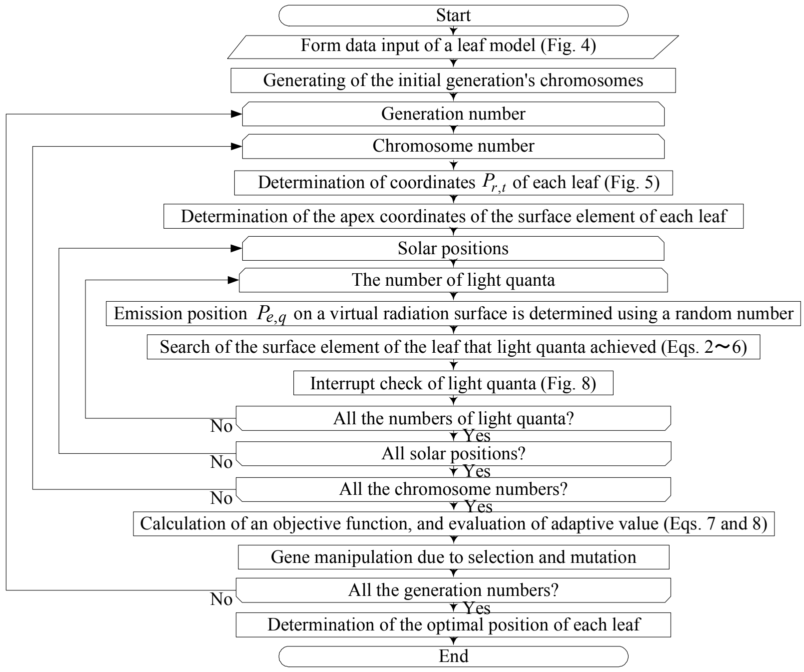


Fig. 10  Calculation flow of LAPS

When the real number is expressed with a 10-bit binary number, the analytical error is 1% or less. Here, subscript $i$ expresses the leaf number of a plant shoot, and $J_l$ is the total leaves in the shoot.

The initial generation's chromosome model is determined using random numbers. The generation number given previously is repeated, adding the genetic manipulation described later to the chromosome model. A solution with a high adaptive value is sought via such an operation.

(2) Adaptive value

The adaptive value of the chromosome model is estimated to be high, meaning there are many light quanta arriving to each leaf. The adaptive value is calculated using Eq. (8). In the last generation's chromosome model, an individual with the highest adaptive value is considered the optimal solution. By decoding the gene of this model, the configuration of a shoot ( $\theta_i$ , $\varphi_i$ , $\beta_i$ , $r_i$ ) is obtained.

3.5 Analysis flow

Figure 10 shows the analysis flow of LAPS used for this study. First, the form data (Fig. 4) of a leaf model, the generation number, and the parameters used for GA are input. Next, the initial generation's chromosome models (Fig. 9) are randomly generated. The reference point $P_{r,t}$ of the leaf shown in Figs. 4 and 5 is decided by decoding the chromosome. Moreover, the radiation position $P_{e,q}$ of the light quantum on the virtual radiation surface is determined using the Monte Carlo calculation. The path of the light quantum is determined by calculating the normal line vector of this radiation position (Fig. 6). The virtual radiation surface changes position during each sampling so that the solar position may be simulated. Based on Eqs. (2)-(7), the surface element number of the leaf that a light quantum reaches is obtained. If the number of light quanta that reach all the leaves is found, the fitness value of each chromosome model can be obtained from Eqs. (8) and (9).

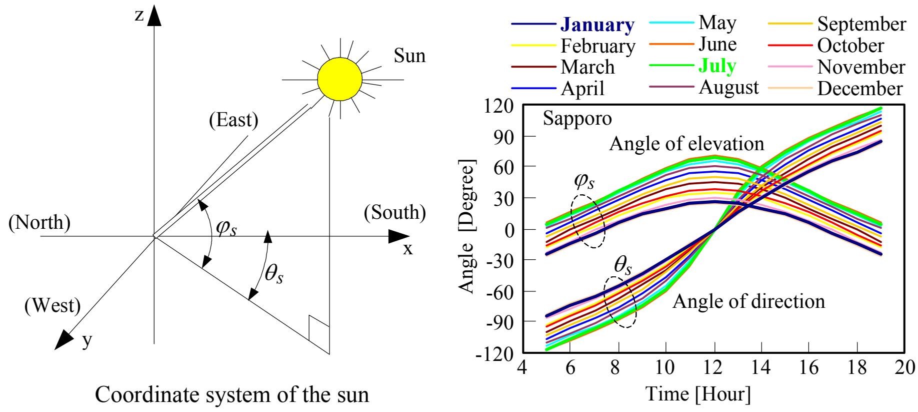


Fig. 11 Position of the sun

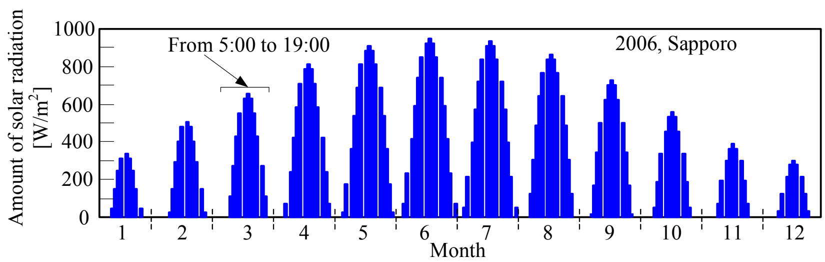


Fig. 12 The amount of solar radiation on the horizontal plane

Mutation is added to the high chromosome group. Furthermore, new chromosomes decided at random are added and a next-generation chromosome group is generated. The last generation is input beforehand and the above calculation is repeated. In the last generation's chromosome model group, the individual with the highest fitness value is decided on as the optimal solution. The optimal arrangement of the plant shoot can be obtained by decoding the optimal solution.

## 4. Analysis conditions

4.1 Parameters of GA

Based on trial and error, the parameters were set up in the analysis as follows. The number of light quanta emitted daily from the virtual radiation surface is 20000, and 100 chromosome models are used. The number of light quanta is distributed in proportion to the amount of insolation during the sampling period. Genetic manipulation is restricted to mutation, and the mutation probability is 0.2. In a mutation, 10% or less of the gene is reversed at random. Moreover, the generation number is 30.

4.2 Conditions of the plant shoot configuration

The analysis system (Figs. 2, 5, 6) is taken as the mirror symmetry of the x-z plane. The total $J_l$ of a leaf is set to four, and all leaf shapes and sizes are identical (Fig. 4). The length of a leaf branch is 0, 50, 100, or 150mm, and the central line of the leaf branch and the costa of the leaf are fixed at right-angles. To facilitate the analysis, the plant shoot configuration is set up under the following constraints:

$$-120\ \text{degree} \le \theta \le 120\ \text{degree} \quad (10)$$

$$0\ \text{degree} \le \varphi \le 120\ \text{degree} \quad (11)$$

$$0\ \text{degree} \le \beta \le 90\ \text{degree} \quad (12)$$

4.3 Light source

The virtual radiation surface is taken as a 1 m square. Using this size, the entire shoot can be reached by the light quanta. The coordinates of the center of the virtual radiation surface

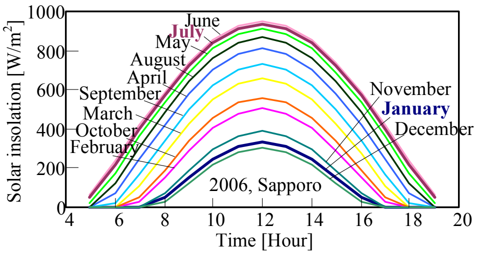


Fig. 13 Insolation of the level surface

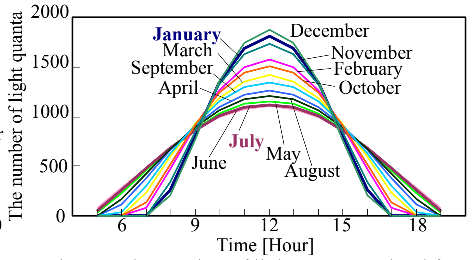


Fig. 14 The number of light quanta emitted from the virtual radiation plate

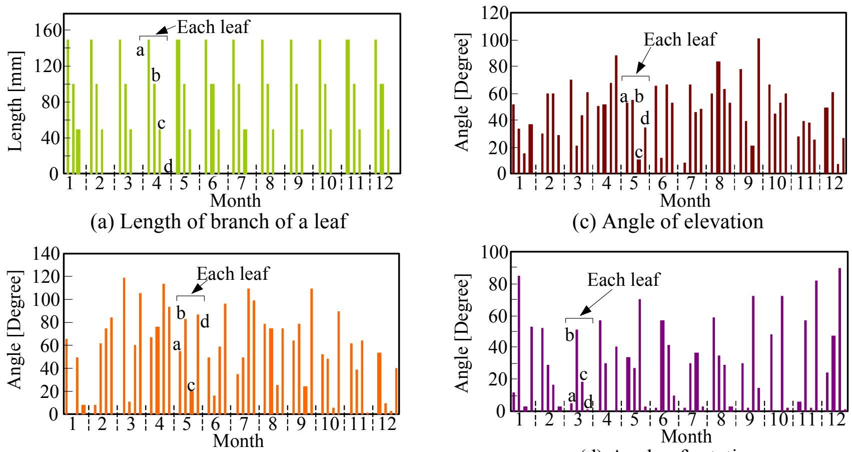


(a) Length of branch of a leaf
(c) Angle of elevation
(b) Angle of direction
(d) Angle of rotation

Fig. 15 Analysis results of the optimal form of the shoot

are set as the solar position (the direction angle $\theta_s$ and the angle of elevation $\varphi_s$). For this paper, the system is assumed to be installed in Sapporo, Japan. Moreover, the number of light quanta for every sampling time emitted from the virtual radiation surface is determined using Eq. (1). The reflection and transmission by the leaf are excluded in this analysis.

4.4 Solar position and the amount of global solar radiation

Figure 11 shows the solar position for every month (half month) in Sapporo [6]. The definitions of the angles of direction and elevation are shown in this figure. On the representative day in the middle of the summer season, the solar elevation and direction angles vary widely. Figure 12 shows the time averaged value of the level surface global solar radiation for every month of 2006 [7]. There are 14 daylight hours in May to July, from 5:00 to 19:00. On the other hand, there are 8 daylight hours in January, November, and December, from 8:00 to 16:00. The amounts of global solar radiation in March, September, and December are 54%, 63%, and 19%, respectively, of that for a representative day in June.

## 5. Analysis results

5.1 The number of light quanta to be emitted

As described in Section 3.1 (2), the number of light quanta emitted for each sampling time is proportional to the extent of global solar radiation shown in Fig. 13, and calculated from Eq. (1). When Eq. (1) is calculated by setting $N_a$ to 20000, the number of light quanta emitted from the virtual radiation surface has the characteristics of Fig. 14. The peak emission will be at 12:00 in all months, and the winter peak is higher. During the summer, although the peaks are low, they include wide ranges. The ranges for the winter are narrow, and there is little emission of light in the morning and evening. It is expected that the leaves (acceptance surface) of the plant shoots will be arranged so that their direction during the summer may facilitate the wider collection of light.

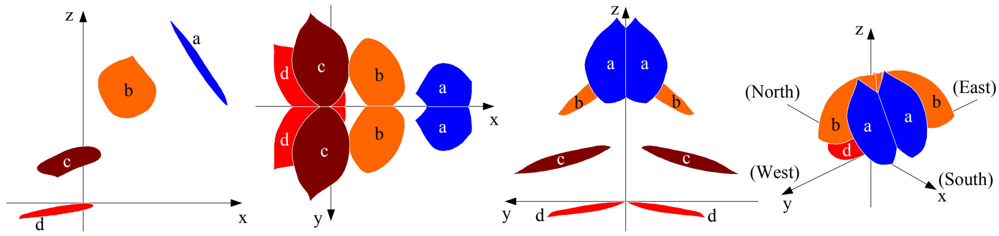


(a) x-z plane (b) x-y plane (c) y-z plane (d) Conformal map

Fig. 16 Result of the optimal arrangement of the leaf in July

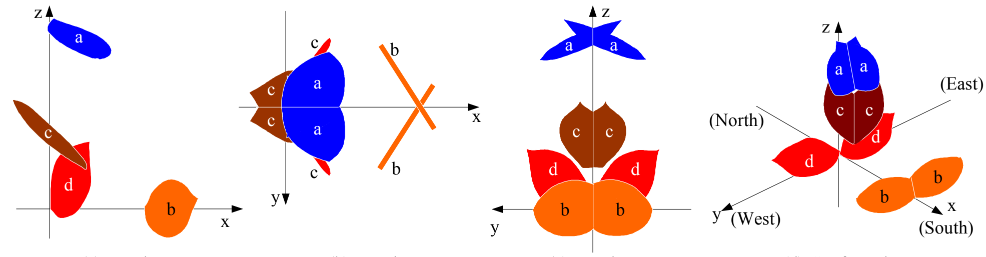


(a) x-z plane (b) x-y plane (c) y-z plane (d) Conformal map

Fig. 17 Result of the optimal arrangement of the leaf in January

5.2 Optimal configuration of shoot

Figs. 15 (a) to (d) show the optimal shoot configurations for every month. As shown in Fig. 15 (a), the length of leaf branches a, b, c, d is 150mm, 100mm, 50mm, and 0mm. As shown in Fig. 15 (b) to (d), even if the shoot configuration is compared on a monthly basis, it is difficult to find regularity. This is because two or more solutions similar to the optimal solution are obtained.

Figures 16 and 17 show the results of the optimal arrangement of the leaves of the plant shoot in July and January. During the summer season, the solar position significantly influences the elevation angle, and the surfaces of all leaves turn to a high position. However, in winter, the arrangement changes such that half the overall number of leaves (Leaves b and c in Fig. 17) may absorb solar radiation with a small angle of elevation.

5.3 Characteristics of the light received

Figure 18 shows the number of light quanta received by the plant shoot based on the analysis results shown in Fig. 15. A greater volume of light is received in winter than in summer. On the other hand, regularity of the volume of light received by the length of the leaf branch is not found. In order to investigate the details, the volume of light received by each leaf for each period of the representative days in January and July was analyzed (Fig. 19). Fig. 20 shows the number of light quanta received by all leaves in a representative day for each month. The volume of light received will differ significantly in July and January because the range of the elevation and direction angles of the sun in July is greater than in January. Therefore, in order to obtain the amount of solar radiation within a wide range, leaves must be arranged in various orientations. As shown in Fig. 13, the solar radiation will peak at 12:00. The amount of solar radiation obtained at 12:00 and the amount of solar radiation when leaves have been arranged in various orientations are compared, and the optimal arrangement is determined. As shown in Fig. 16 (b), the results show that the configuration was strongly influenced by the solar position at 12:00. Accordingly, all the leaves face upward. However, because the solar radiation at 12:00 is relatively weak compared with other periods, the leaf arrangements will be subject to variation in January.

5.4 Directivity

In order to investigate directivity, a shoot with four leaves arranged parallel to the x-y plane was analyzed as shown in Fig. 21. The direction angles $\theta$ of each shoot were 0, 30, 60, and 90 degrees, the elevation angle of all the shoots was 90 degrees, while the length of

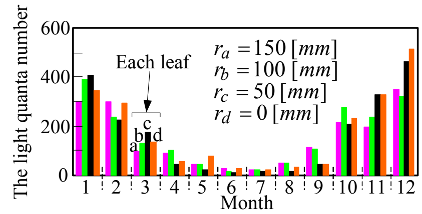


Fig. 18 Light quanta receiving number of each leaf

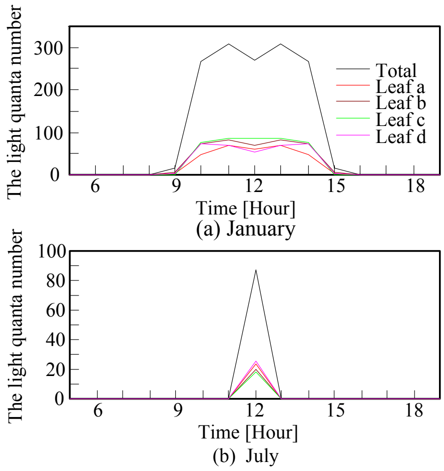


Fig. 19 The number of reaching of the light quantum in each leaf

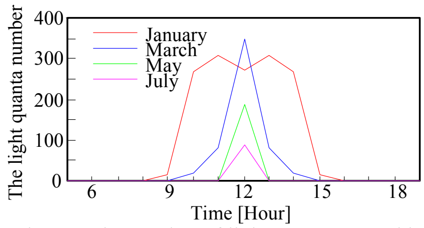


Fig. 20 The number of light-quantum reaching in all the leaves

a leaf branch (= height in the direction of z axis) was 0, 50, 100, and 150mm. The result of the optimal monthly configuration is compared with the volume of light received based on this arrangement. The optimal configuration of the monthly plant shoot and the result of having arranged the leaf in parallel with the x-y plane described above are shown in Fig. 22. The difference of the leaves arranged parallel with the x-y plane between March and September and the leaves of the optimal arrangement is small. However, significant greater volumes of light are received with the optimal arrangement of leaves for five months; namely January, February, and October to December. As described in Section 5.3, during the summer period, the leaves are optimized in the solar position at 12:00 when there is a significant angle of elevation. Therefore, the difference in the amount of light received for the leaves arranged parallel with the x-y plane and the optimal arrangement is small. On the other hand, the optimal arrangement of the leaves in January, February, and October to December involves a considerable volume of light being received within a wide time period, as shown in Fig. 20. Therefore, the arrangement of the leaves in this case has small directivity. The relation between the directive strength of a plant shoot and the volume of light received by the leaves differs greatly in terms of the magnitude of the solar movement zone and the global solar radiation in sampling time.

5.5 Installation space

Figure 23 shows the shoot configuration in January and July (Figs. 16 and 17), and the arrangement of the leaves shown in Fig. 21 on the same coordinate system. The installation space needed for each shoot configuration can be compared from this figure. When the installation space of the leaves in Fig. 21 and those in Figs. 16 and 17 are compared, those in Figs. 16 and 17 are not necessarily minimized. However, if the length of the branches of a leaf and the size of the leaves are expressed in the chromosome model of GA and the objective function of the miniaturization is given, a smaller shoot configuration of the installation space will be expected. The miniaturization of the installation space was not a focus of this paper.

## 6. Conclusions

The relation between the configuration a plant shoot and the amount of light received is investigated, and the distribution of solar modules using this configuration is planned. This study will facilitate a power generation system with a small installation space and weak directivity. With this in mind, the relation between the shoot configuration of a dogwood and the amount of light received was investigated using the light received analysis

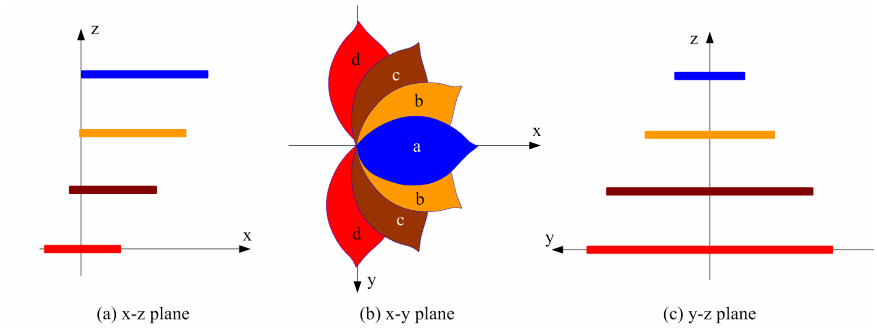


Fig. 21 The leaves set horizontally

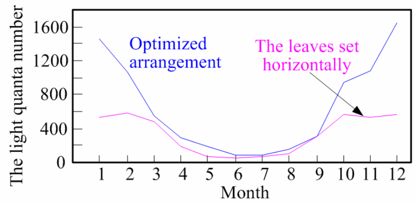


Fig. 22 Light quanta receiving number in every month

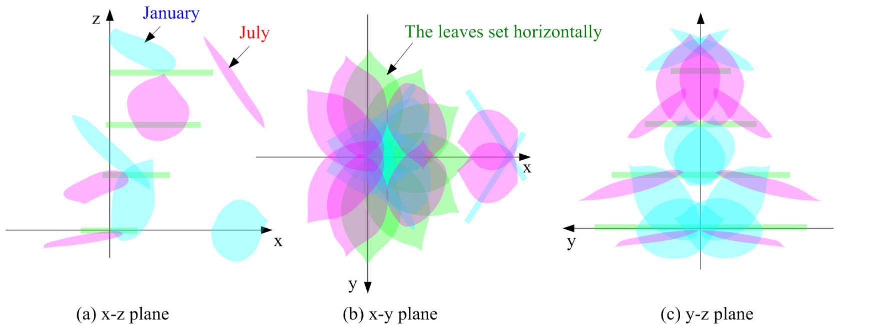


Fig. 23 Comparison of the shoot configuration

algorithm of a plant shoot (LAPS), via the Monte Carlo method and a genetic algorithm. The following conclusions were obtained:

(1) Because the range of the solar angle of elevation and direction angle in the summer season is wide, leaves should be arranged so that the solar radiation may be received in a wide range. Solar radiation will peak in summer at 12:00. The amount of solar radiation obtained around 12:00 and the amount of solar radiation when leaves are variously arranged are compared, and the optimal arrangement of the shoot is determined. Based on the analysis results, a configuration strongly influenced by the solar position around 12:00 was shown. However, the optimal arrangement in winter differs from that in summer in various ways.

(2) When the volume of light received of when the leaves are arranged horizontally and the configuration of the optimal plant shoot is measured, the difference will be modest for the March to September period. However, a greater amount of light will be received for a plant shoot optimized in space in January, February, and October to December than if the leaves are arranged horizontally.

## Nomenclature

| | | |
|---|---|---|
| $E_{w,k}$ | : | The number of light quanta that reached the surface element $k$ in Leaf $w$ |
| $e$ | : | Level surface global solar radiation |
| $J_e$ | : | The number of the leaf-surface-elements |
| $J_l$ | : | The number of the leaves |
| $\overrightarrow{N}$ | : | Normal line vector of the leaf model |

| | | |
|---|---|---|
| $N_a$ | : | The total number of light quanta emitted in a day |
| $nq$ | : | The number of light quanta to emit |
| $P$ | : | Point in the coordinate system |
| $P_e$ | : | Coordinates of the radiation position on the virtual radiation surface |
| $P_{le}$ | : | Apex coordinates of the surface element of a leaf |
| $P_r$ | : | Corner point of the central line in the leaf model (Fig. 4) |
| $P_s$ | : | Apex coordinates of a surface element of the leaf |
| $P_t$ , $P_u$ | : | Coordinates of the light quantum arriving on the leaf |
| $P_v$ | : | Apex coordinates of a virtual radiation surface |
| $\dot{q}_d$ | : | Coordinates of the light quantum that reached directly from the virtual radiation surface |
| $\dot{q}'_h$ | : | Coordinates of the light quantum that reaches after transmitting from other leaves |
| $R_{g,st}$ | : | The rate emitted to $st$ among $N_a$ |
| $r$ | : | Length |
| $r_{et}$ | : | Length between $P_{e,q}$ and $P_{t,m}$ (Fig. 8) |
| $r_{lt}$ | : | Length showing the apex of the leaf model (Fig. 4) |
| $\vec{V_e}$ | : | Normal line vector of $P_e$ |

Roman character

| | | |
|---|---|---|
| $\alpha$ | : | Absorptivity |
| $\beta$ | : | Angle of rotation (degree) |
| $\varepsilon$ | : | Content of photosynthesis enzyme |
| $\varphi$ | : | Angle of elevation (degree) |
| $\gamma$ | : | Reflectivity |
| $\eta_{t,x,m}$ | : | Angle of the central line on the leaf, and the apex $x$ of element $m$ (Fig. 4) (degree) |
| $\theta$ | : | Angle of direction (degree) |
| $\tau$ | : | Transmissivity |

Subscript

| | | |
|---|---|---|
| $a$ , $b$ | : | Light-quantum number that reached the leaf directly from the virtual radiation surface |
| $g$ | : | Representative month |
| $i$ , $j$ | : | Number of the leaf model |
| $k$ , $m$ , $n$ | : | Surface element number of the leaf |
| $q$ | : | Simulated light-quantum number |
| $s$ | : | Sun |
| $st$ | : | Sampling time |
| $t$ , $u$ , $w$ | : | Number of the leaf model |
| $x$ | : | Apex number of the surface element of a leaf |

## References


(1) The Society for the Study of Species Biology, *Figures of Light, Water, and a Plant -Guide to Plant Physiological Ecology*, （2003）, .Bun-ichi Sogo Shyuppan.

(2) Shin'ya OBARA and Itaru TANNO, Arrangement Analysis of Leaves Optimized on Photon Flux Density or Photosynthetic Rate, *Journal of Computational Science and Technology*, 2(1), 118-129, (2008).

(3) Takashi Minemoto and Hideyuki Takakura, Fabrication of Spherical Silicon Crystals by Dropping Method and Their Application to Solar Cells, Jpn. J. Appl. Phys., **46**, 7A, 4016-4020 (2007).

(4) Bifacial Photovoltaic Solar Module "SOLAZURE Series", *Hitachi Ronpyo*, **2**, 61-62 (2006).

(5) Hiroshi Taniguchi, et. al., *Radiant-Heat-Transfer Analysis Using the Monte Carlo Method of Personal Computer Utilization*, (1993), Corona Publishing Co., Ltd.

(6) National Astronomical Observatory, “Rika Nenpyo” Chronological Scientific Tables CD-ROM, (2003), Maruzen Co., Ltd.

(7) Homepage of Japan Meteorological Agency, http://www.data.jma.go.jp/obd/stats/etrn/index.php, (2007).